Available online at www.sciencedirect.com
ScienceDirect
Digital Signal Processing 18 (2008) 777–796
Digital Signal Processing
www.elsevier.com/locate/dsp

Noncircularity-exploitation in direction estimation of noncircular signals with an acoustic vector-sensor

Yougen Xu *, Zhiwen Liu

Department of Electronic Engineering, Beijing Institute of Technology, Beijing, People's Republic of China

Available online 1 November 2007

Abstract

The main motivation of using an acoustic vector-sensor in direction-of-arrival (DOA) estimation applications has been its unambiguous two-dimensional directivity, insensitivity to the range of sources, and independence of signal frequency. The main objection lies in its lack of geometry-redundancy and limited degree of freedom. Four thus emerged challenging tasks and the corresponding solutions by recurring to the redundancies in the nonvanishing conjugate correlations of noncircular signals are described in the paper: (1) fulfilling source decorrelation in a multipath propagation environment; (2) enhancing processing capacity to accommodate more signals; (3) suppressing colored-noise with unknown covariance structure; and (4) deriving closed-form approaches to avoid iteration and manifold storage. Simulation experiments are carried out to examine the associated DOA estimators termed as: (1) phase-smoothing MUSIC (multiple signal classification); (2) virtual-MUSIC; (3) conjugate-MUSIC; and (4) noncircular-ESPRIT (estimation of signal parameters via rotational invariance techniques), respectively.

Keywords: Antenna arrays; Array signal processing; Direction-of-arrival estimation

1. Introduction

Over the last decade, numerous algorithms have been developed for the problem of DOA estimation of signals with acoustic vector-sensors [1–8], though, mostly repeat the work accomplished for the scalar-sensor counterparts. A "complete" acoustic vector-sensor such as a vector-hydrophone consists of a pressure sensor and a collocated triad of three orthogonal velocity sensors. These four sensors together measure the scalar acoustic pressure and all three components of the acoustic particle velocity vector of the incident wave-field at a given point [1]. In contrast, an "incomplete" acoustic vector-sensor consists of a subset of the above four-component sensors, for example, a three-component hydrophone formed from two orthogonally oriented velocity hydrophones and a pressure hydrophone [5]. The scalar-sensor such as a pressure-hydrophone thus can also be viewed as a special incomplete acoustic vector-sensor. In this paper, we only consider the complete acoustic vector-sensor.

The angular diversity present in even a single acoustic vector-sensor results in an effective aperture for the task of DOA estimation. An acoustic vector-sensor may be treated as a special array comprising four or less elements, and it has been shown in [9] that two signals can be uniquely identified by a complete acoustic vector-sensor. In addition,

* Corresponding author.
E-mail address: yougenxu@bit.edu.cn (Y. Xu).

1051-2004/$ – see front matter
doi:10.1016/j.dsp.2007.10.008

the array manifold of an acoustic vector-sensor is frequency-independent and hence the attendant DOA estimation algorithms are insensitive to the signal bandwidth. Another interesting feature of uni-vector-sensor array manifold is its realness nature. Still, unambiguous 2D DOA estimation (joint estimation of azimuth and elevation angles) can be accomplished with merely one acoustic vector-sensor.

However, due to its limited degree of freedom and lack of sensor-doublets, uni-vector-sensor based DOA estimation may encounter great difficulties in several important practical applications such as multipath propagation, heavy co-channel interferers, and colored-noise contamination, etc. Moreover, scalar-sensor counterparts for solving these mentioned problems do not seem to be available since most existing schemes devised for scalar-sensor arrays require the use of sensor-doublets or impose certain constraints on sensor arrangement—both of which are impossible for the case of an acoustic vector-sensor. Thus, developing effective DOA estimation algorithms especially for the aforementioned practical considerations is of critical importance for the popularity of using one vector-sensor for DOA estimation. To this end, we herein discuss the subspace-based methods for uni-vector-sensor DOA estimation, with focus on the next four topics: (1) aperture-preservable source decorrelation in a multipath propagation environment; (2) increasing the number of uniquely identified signals; (3) colored-noise cancellation; and (4) iteration-free approaches to reduce computation load, by recognizing and exploiting underlying noncircularity of noncircular signals such as rectilinear AM (amplitude modulated) and BPSK (binary phase shift keying) signals. During the last two decades, there has been an increasing interest in employing phase-coherent modulation techniques in underwater wireless communication systems. Phase-coherent PSK signals were demonstrated to be a viable way of achieving higher bandwidth efficiency over many of the underwater channels [27–29], which served as another motivation behind the present work. Some pioneering work on noncircularity exploitation in DOA estimation with scalar-sensors instead of vector-sensors can be found in [10–13].

The rest of the paper is organized as follows. In Section 2, we introduce the data model. In Section 3, we propose the phase-smoothing technique for DOA estimation of two coherent signals. We then present in Sections 4, 5, and 6 the virtual-MUSIC (for localizing more than two signals), the conjugate-MUSIC (for colored-noise suppression), the noncircular-ESPRIT (be close-form in nature), respectively. The simulation results are finally given in Section 7. Throughout the paper, we denote matrices and vectors by bold uppercase and bold lowercase letters. Superscripts "T," "H," and "*" stand for transpose, conjugate transpose, and conjugate, respectively. $\mathbf{I}_{M,N}$ and $\mathbf{O}_{M,N}$ denotes the $M \times N$ identity matrix and zero matrix, respectively. We will suppress the index when this does not lead to any confusion. Moreover, "$\mathbf{0}$" denotes zero vector, "E" denotes statistical expectation.

2. Statistical data model

2.1. Vector-sensor measurements

It is assumed that the acoustic wave is traveling in a quiescent, homogeneous, and isotropic fluid, and is from a source of azimuth θ and elevation ϕ, where $0 \leqslant \theta < 2\pi$ and $0 \leqslant \phi \leqslant \pi$ are respectively measured from the positive x-axis and the positive z-axis (see Fig. 1). Then, the "complete" acoustic vector-sensor's 4×1 array response vector in a free space equals [1]:

$$\mathbf{a}(\theta,\phi) = \begin{pmatrix} \cos(\theta)\sin(\phi) \\ \sin(\theta)\sin(\phi) \\ \cos(\phi) \\ 1 \end{pmatrix} = \begin{pmatrix} u_x \\ u_y \\ u_z \\ 1 \end{pmatrix}, \tag{1}$$

where u_x, u_y, and u_z are the direction cosines along the x-, y-, and z-axis, respectively. The above two-dimensional azimuth-elevation directivity is inherently real-valued and independent of signal frequency and hence signal bandwidth. The array manifold for an acoustic vector-sensor is defined as $\mathcal{M} = \{\mathbf{a}(\theta,\phi)\colon\ (\theta,\phi) \in \Theta\}$, where Θ is the entire field of view.

2.2. Noncircular signal model

Assume that Q acoustic signals impinge upon the acoustic vector-sensor, then the vector-sensor output is given by

$$\mathbf{r}(t) = \sum_{p=1}^{Q} \mathbf{a}_p s_p(t) + \mathbf{n}(t) = \mathbf{A}\mathbf{s}(t) + \mathbf{n}(t), \tag{2}$$

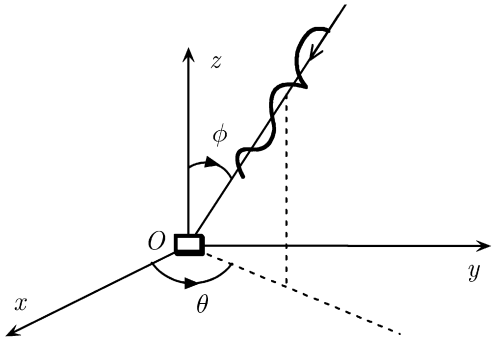

Fig. 1. Coordinate system and angle definition.

where $\mathbf{a}_p = \mathbf{a}(\theta_p, \phi_p)$, $\mathbf{A} = [\mathbf{a}_1, \ldots, \mathbf{a}_Q]$, $\mathbf{s}(t) = [s_1(t), \ldots, s_Q(t)]^T$ is the signal vector, and $E(s_p^2(t)) \neq 0$ for $p = 1, 2, \ldots, Q$ (all the signals are noncircular), and $\mathbf{n}(t)$ is the additive noise term. It is assumed that

- $E(s_p^2(t)) = \mu_p e^{j\vartheta_p} E(|s_p(t)|^2) = \mu_p e^{j\vartheta_p} \sigma_{s,p}^2$, $\mu_p = 1$ (the circularity rate over [0, 1]);
- $E(\mathbf{n}(t)\mathbf{n}^H(t)) = \sigma_n^2 \mathbf{I}$, $E(\mathbf{n}(t)\mathbf{n}^T(t)) = \mathbf{O}$;
- $E(\mathbf{n}(t)s_p(t)) = \mathbf{0}$, $E(\mathbf{n}(t)s_p^*(t)) = \mathbf{0}$.

A signal $s(t)$ is said to be noncircular if $\mu \neq 0$ and, hence $E(s^2(t)) \neq 0$ [10]. In other words, a noncircular signal has nonvanishing conjugate correlation in addition to nonzero correlation. This statistics redundancy may be properly exploited for overcoming some serious problems in one vector-sensor based DOA estimation. In the above, we have assumed that all the signals to be processed are noncircular. More specifically, if all the signals have linear constellations, e.g., the BPSK signal, the AM signal [11–13] (also known as rectilinear signal), then the baseband signals may be expressed as $s_p(t) = e^{j\varphi_p} s_{r,p}(t)$, where $\varphi_p = \frac{1}{2}\vartheta_p$ denotes the arbitrary and possibly unknown initial phase of the pth incident signal, and $s_{r,p}(t) = s_{r,p}^*(t)$. As a consequence, we have $\mathbf{s}(t) = \mathbf{\Phi}\mathbf{s}_r(t)$ and, hence

$$\mathbf{r}(t) = \mathbf{A}\mathbf{\Phi}\mathbf{s}_r(t) + \mathbf{n}(t), \tag{3}$$

where $\mathbf{\Phi} = \operatorname{diag}(e^{j\varphi_1}, \ldots, e^{j\varphi_Q})$ with $e^{j\varphi_p} \neq e^{j\varphi_q}$ for $p \neq q$, while $\mathbf{s}_r(t)$ is the real signal vector which is defined as $\mathbf{s}_r(t) = [s_{r,1}(t), \ldots, s_{r,Q}(t)]^T$, and $\mathbf{s}_r^*(t) = \mathbf{s}_r(t)$. Unless otherwise mentioned, we will specialize to rectilinear signals in what follows.

3. Source decorrelation for two coherent signals

In this section, we address the problem of DOA estimation of coherent signals by using MUSIC-like method [15]. To uniquely determine DOAs of K uncorrelated sources, it is required by the standard MUSIC that every $K + 1$ steering vectors of distinct DOAs are linearly independent. It was verified in [9] that every *three* steering vectors of an acoustic vector-sensor (defined in (1)) with distinct DOAs are linearly independent, thereby enabling unambiguous DOA estimation of two uncorrelated signals by using the standard MUSIC. In the presence of two coherent signals, however, the standard MUSIC would become fail due to the rank-deficient problem of the source correlation matrix.

3.1. Rank-deficient problem

Consider two coherent noncircular signals impinge upon the aforementioned acoustic vector-sensor. Denote the two signals as $s_1(t)$ and $s_2(t)$, where $s_1(t) = e^{j\varphi_1} s_r(t)$, $s_2(t) = \rho e^{j\varphi_2} s_r(t)$, and $\rho \neq 0$ is the relative attenuation factor (here ρ is a real integer since the relative phase between the two coherent signals may be absorbed into φ_2). The output of an acoustic vector-sensor then becomes ($Q = 2$):

$$\mathbf{r}(t) = \sum_{p=1}^{2} \mathbf{a}(\theta_p, \phi_p) s_p(t) + \mathbf{n}(t) \tag{4}$$

and the array covariance matrix is given by

$$\mathbf{R}_r \stackrel{\text{def}}{=} E\big(\mathbf{r}(t)\mathbf{r}^H(t)\big) = \underline{\mathbf{A}}\,\underline{\mathbf{R}}_s\underline{\mathbf{A}}^H + \sigma_n^2\mathbf{I}, \tag{5}$$

where $\underline{\mathbf{A}} = [\mathbf{a}(\theta_1,\phi_1), \mathbf{a}(\theta_2,\phi_2)]$ (the underlined symbol here is used to designate that the quantity is associated with only two signals), and, as usual, the source subspace is defined as span($\underline{\mathbf{A}}$) which is dependent on the two DOAs to be estimated. In addition,

$$\underline{\mathbf{R}}_s \stackrel{\text{def}}{=} E\big(\underline{\mathbf{s}}(t)\underline{\mathbf{s}}^H(t)\big) = \underbrace{E\big(s_r^2(t)\big)}_{\stackrel{\text{def}}{=}\sigma_s^2}\begin{pmatrix} e^{j\varphi_1} \\ \rho e^{j\varphi_2}\end{pmatrix}\begin{pmatrix} e^{j\varphi_1} \\ \rho e^{j\varphi_2}\end{pmatrix}^H \tag{6}$$

is the source covariance matrix with $\underline{\mathbf{s}}(t) = [s_1(t), s_2(t)]^T$. By definition, $\operatorname{rank}(\underline{\mathbf{R}}_s) = 1 < Q = 2$ which is referred to as the rank-deficient problem [14].

Eigendecompose $\mathbf{R}_r$ to obtain

$$\mathbf{R}_r = \zeta_s\mathbf{u}_s\mathbf{u}_s^H + \sigma_n^2\mathbf{V}_n\mathbf{V}_n^H, \tag{7}$$

where $\zeta_s > \sigma_n^2$. The signal subspace and the noise subspace are then respectively defined as span($\mathbf{u}_s$) and span($\mathbf{V}_n$), and

$$\begin{cases} \operatorname{span}(\mathbf{V}_n) \perp \operatorname{span}(\mathbf{u}_s), \\ \mathbf{V}_n\mathbf{V}_n^H = \mathbf{I} - \mathbf{u}_s\mathbf{u}_s^H. \end{cases} \tag{8}$$

Since $\mathbf{R}_r = \sigma_s^2\mathbf{b}_{1,2}\mathbf{b}_{1,2}^H + \sigma_n^2\mathbf{I}$, where $\mathbf{b}_{1,2} = e^{j\varphi_1}\mathbf{a}(\theta_1,\phi_1) + \rho e^{j\varphi_2}\mathbf{a}(\theta_2,\phi_2)$, we have $\operatorname{span}(\mathbf{u}_s) = \operatorname{span}(\mathbf{b}_{1,2})$.

Generally, $\operatorname{span}(\mathbf{u}_s) \subset \operatorname{span}(\underline{\mathbf{A}})$, $\mathbf{b}_{1,2} \notin \mathcal{M}$ (the array manifold of an acoustic vector-sensor as has defined earlier). Then, both $\mathbf{a}(\theta_1,\phi_1)$ and $\mathbf{a}(\theta_2,\phi_2)$ are not orthogonal to the noise subspace. As a consequence, the MUSIC algorithm [15] will degrade seriously or even fail. More exactly, the pseudo-MUSIC spectrum defined as

$$f_{\text{MU}}(\theta,\phi) = \frac{\mathbf{a}^H(\theta,\phi)\mathbf{a}(\theta,\phi)}{\mathbf{a}^H(\theta,\phi)\mathbf{V}_n\mathbf{V}_n^H\mathbf{a}(\theta,\phi)} \tag{9}$$

generally will not exhibit peaks at the position of the two true DOAs, i.e., (θ_1,ϕ_1), (θ_2,ϕ_2), due to the collapse of signal subspace.

A well-known source decorrelation method is the spatial smoothing technique [14]. However, the spatial smoothing technique requires translationally invariant subarrays—a condition often violated in an acoustic vector-sensor. Another possible measure is through maximum likelihood method but it is computationally intensive. We next suggest two computationally effective methods to cope with the coherency problem for an acoustic vector-sensor only. The main idea behind our method is to restore the rank property of source covariance matrix through the so-called phase smoothing.

3.2. Direct phase-smoothing

To recover the rank property of the source covariance matrix $\underline{\mathbf{R}}_s$, we perform the next averaging termed as phase smoothing:

$$\mathbf{R}' = \frac{1}{2}\big(\mathbf{R}_r + \mathbf{R}_r'\big), \tag{10}$$

where $\mathbf{R}_r' = E(\mathbf{r}^*(t)\mathbf{r}^T(t)) = (\mathbf{R}_r)^*$ is the conjugate of array covariance matrix $\mathbf{R}_r$ defined above. It follows that

$$\mathbf{R}' = \frac{1}{2}\big(\mathbf{R}_r + \mathbf{R}_r'\big) = \frac{1}{2}\big(\underline{\mathbf{A}}\,\underline{\mathbf{R}}_s\underline{\mathbf{A}}^H + \mathbf{A}(\underline{\mathbf{R}}_s)^*\underline{\mathbf{A}}^H + 2\sigma_n^2\mathbf{I}\big) = \underline{\mathbf{A}}\underbrace{\frac{1}{2}\big(\underline{\mathbf{R}}_s + \underline{\mathbf{\Phi}}\,\underline{\mathbf{R}}_s\underline{\mathbf{\Phi}}^H\big)}_{\stackrel{\text{def}}{=}\bar{\mathbf{R}}_s}\underline{\mathbf{A}}^H + \sigma_n^2\mathbf{I} = \underline{\mathbf{A}}\bar{\mathbf{R}}_s\underline{\mathbf{A}}^H + \sigma_n^2\mathbf{I}, \tag{11}$$

where $\underline{\mathbf{\Phi}} = \operatorname{diag}(e^{-j2\varphi_1}, e^{-j2\varphi_2}) = \mathbf{\Phi}^{-2}$, and

$$\bar{\mathbf{R}}_s = \frac{\sigma_s^2}{2}\left[\begin{pmatrix} 1 & \rho e^{-j\Delta\varphi} \\ \rho e^{j\Delta\varphi} & \rho^2\end{pmatrix} + \begin{pmatrix} 1 & \rho e^{j\Delta\varphi} \\ \rho e^{-j\Delta\varphi} & \rho^2\end{pmatrix}\right] = \sigma_s^2\begin{pmatrix} 1 & \rho\operatorname{Re}(e^{j\Delta\varphi}) \\ \rho\operatorname{Re}(e^{j\Delta\varphi}) & \rho^2\end{pmatrix}, \tag{12}$$

where $\Delta\varphi = \varphi_2 - \varphi_1$. Note that $\det(\bar{\mathbf{R}}_s) = \sigma_s^2\rho^2\sin^2\Delta\varphi$, then $\operatorname{rank}(\bar{\mathbf{R}}_s) = 2$ so long as $\Delta\varphi \neq k\pi$, where $k = 0, \pm1, \pm2$. Hence, the rank property can be restored by phase smoothing.

It is interesting to note that the decorrelation performance of phase smoothing is independent of the DOAs of coherent signals. This is quite different from the conventional spatial smoothing scheme that behaves fairly poor when the DOAs of coherent signals become very close [16]. Another difference between phase smoothing and spatial smoothing is that the former does not involve any aperture loss.

3.3. Squared phase-smoothing

The direct phase smoothing suggested above exploits only the correlations of data. To utilize both correlations and conjugate correlations, we now describe a modified phase smoothing scheme. First, we define the following so-called squared array covariance matrix:

$$\mathbf{R}_r^2 = \mathbf{R}_r^H\mathbf{R}_r = \underline{\mathbf{A}}\underbrace{\left(\underline{\mathbf{R}}_s^H\underline{\mathbf{A}}^H\underline{\mathbf{A}}\underline{\mathbf{R}}_s\right)}_{\stackrel{\text{def}}{=}\mathbf{Q}_s'}\underline{\mathbf{A}}^H + \sigma_n^2\underline{\mathbf{A}}\left(\underline{\mathbf{R}}_s^H + \underline{\mathbf{R}}_s\right)\underline{\mathbf{A}}^H + \sigma_n^4\mathbf{I} = \underline{\mathbf{A}}\mathbf{Q}_s'\underline{\mathbf{A}}^H + 2\sigma_n^2\underline{\mathbf{A}}\underline{\mathbf{R}}_s\underline{\mathbf{A}}^H + \sigma_n^4\mathbf{I}, \tag{13}$$

the conjugate array covariance matrix:

$$\mathbf{R}_{r^*} = E\left(\mathbf{r}(t)\mathbf{r}^T(t)\right) = \underline{\mathbf{A}}\underline{\mathbf{R}}_s\underline{\boldsymbol{\Phi}}^H\underline{\mathbf{A}}^H, \tag{14}$$

and the squared conjugate array covariance matrix:

$$\mathbf{C}_r^2 = \mathbf{R}_{r^*}^H\mathbf{R}_{r^*} = \underline{\mathbf{A}}\left(\underline{\boldsymbol{\Phi}}\underline{\mathbf{R}}_s^H\underline{\mathbf{A}}^H\underline{\mathbf{A}}\underline{\mathbf{R}}_s\underline{\boldsymbol{\Phi}}^H\right)\underline{\mathbf{A}}^H = \underline{\mathbf{A}}\left(\underline{\boldsymbol{\Phi}}\mathbf{Q}_s'\underline{\boldsymbol{\Phi}}^H\right)\underline{\mathbf{A}}^H. \tag{15}$$

In the above derivation, the fact $E(\mathbf{n}(t)\mathbf{n}^T(t)) = \mathbf{O}$ is used.

We then may construct the next squared phase smoothing matrix:

$$\mathbf{C}' = \mathbf{R}_r^2 + \mathbf{C}_r^2 = \underline{\mathbf{A}}\left(\mathbf{Q}_s' + \underline{\boldsymbol{\Phi}}\mathbf{Q}_s'\underline{\boldsymbol{\Phi}}^H\right)\underline{\mathbf{A}}^H + 2\sigma_n^2\underline{\mathbf{A}}\underline{\mathbf{R}}_s\underline{\mathbf{A}}^H + \sigma_n^4\mathbf{I} = \underline{\mathbf{A}}\boldsymbol{\Psi}_s'\underline{\mathbf{A}}^H + \sigma_n^4\mathbf{I}, \tag{16}$$

where

$$\boldsymbol{\Psi}_s' = 2\sigma_s^2\begin{pmatrix} (\lambda^2+\sigma_n^2) & \sigma_n^2\rho e^{-j\Delta\varphi} + \lambda^2\rho\cos\Delta\varphi \\ \sigma_n^2\rho e^{j\Delta\varphi} + \lambda^2\rho\cos\Delta\varphi & (\lambda^2+\sigma_n^2)\rho^2 \end{pmatrix}$$

in which $\lambda^2 = \sigma_s^2\gamma^2(\boldsymbol{\psi})$, $\boldsymbol{\psi} \stackrel{\text{def}}{=} [\varphi_1, \varphi_2, \rho, \theta_1, \theta_2, \phi_1, \phi_2]^T$, and

$$\gamma^2(\boldsymbol{\psi}) = \begin{pmatrix} e^{-j\varphi_1} & \rho e^{-j\varphi_2} \end{pmatrix}\underline{\mathbf{A}}^H\underline{\mathbf{A}}\begin{pmatrix} e^{j\varphi_1} \\ \rho e^{j\varphi_2} \end{pmatrix}. \tag{17}$$

Then we have $\det(\boldsymbol{\Psi}_s') = 4\lambda^2\rho^2\sigma_s^4(\lambda^2 + 2\sigma_n^2)\sin^2\Delta\varphi$, and hence $\operatorname{rank}(\boldsymbol{\Psi}_s') = 2$ so long as $\Delta\varphi \neq k\pi$, where $k = 0, \pm1, \pm2$.

3.4. Phase-smoothing-based DOA estimation

After performing phase smoothing, the spectrum expressions of MUSIC can be modified as

$$f_{\text{PS-MU}}(\theta,\phi) = \frac{\mathbf{a}^H(\theta,\phi)\mathbf{a}(\theta,\phi)}{\mathbf{a}^H(\theta,\phi)\tilde{\mathbf{U}}_n\tilde{\mathbf{U}}_n^H\mathbf{a}(\theta,\phi)}, \tag{18}$$

where $\tilde{\mathbf{U}}_n = [\tilde{\mathbf{u}}_1, \tilde{\mathbf{u}}_2]$, in which $\tilde{\mathbf{u}}_1$ and $\tilde{\mathbf{u}}_2$ are the eigenvectors according to the two smallest eigenvalues of either $\mathbf{R}'$ or $\mathbf{C}'$.

It should be pointed out that the phase smoothing technique cannot be directly extended to the conventional scalar-sensor arrays since for the latter $\underline{\mathbf{A}} \neq \underline{\mathbf{A}}^*$. One possible follow-up research is on incorporating the redundancies in the array geometry (such as a linear uniform array of multiple vector-sensors) to decorrelate more than two coherent signals without nearly identical DOAs.

4. Aperture extension

In this section, we discuss the problem of estimating more than two ($Q > 2$) uncorrelated signals with only one acoustic vector-sensor. The scheme described here is not truly new but follows that in [10,11] which are devised for scalar-sensors instead. First, we construct $\mathbf{y}(t) \overset{\text{def}}{=} [\mathbf{r}^T(t), \mathbf{r}^H(t)]^T$, where $\mathbf{r}(t)$ is defined in (2), then the augmented array covariance matrix may be defined as

$$\mathbf{R}_y = E\big(\mathbf{y}(t)\mathbf{y}^H(t)\big) = \begin{pmatrix} \mathbf{A} \\ \mathbf{A}\mathbf{Q}^* \end{pmatrix} \mathbf{R}_s \begin{pmatrix} \mathbf{A} \\ \mathbf{A}\mathbf{Q}^* \end{pmatrix}^H + \sigma_n^2 \mathbf{I}_{8,8}, \tag{19}$$

where $\mathbf{A} = [\mathbf{a}_1, \ldots, \mathbf{a}_Q]$, $\mathbf{Q} = \operatorname{diag}(e^{j\vartheta_1}, \ldots, e^{j\vartheta_Q}) = \mathbf{\Phi}^2$, $\mathbf{R}_s = E(\mathbf{s}(t)\mathbf{s}^H(t))$ with $\mathbf{s}(t) = [s_1(t), \ldots, s_Q(t)]^T$. In the derivation of (19) we have used the realness nature of the array manifold $\mathcal{M}$ for a single acoustic vector-sensor, i.e., $\mathbf{A} = \mathbf{A}^*$, and, as a consequence, $\mathbf{R}_y$ can be looked as the aforementioned array covariance matrix of an eight-element hypothetic array whose virtual array manifold has the next form (we hereafter label the vectors within this virtual array manifold as the virtual steering vectors):

$$\mathbf{b}(\theta,\phi) = \big[\mathbf{a}^H(\theta,\phi), \mathbf{a}^H(\theta,\phi)e^{j\vartheta}\big]^H = \underbrace{\begin{pmatrix} 1 \\ e^{-j\vartheta} \end{pmatrix}}_{\overset{\text{def}}{=}\tilde{\mathbf{h}}(\vartheta)} \otimes \mathbf{a}(\theta,\phi) = \underbrace{\big[\mathbf{I}_{2,2} \otimes \mathbf{a}(\theta,\phi)\big]}_{\overset{\text{def}}{=}\tilde{\mathbf{B}}(\theta,\phi)} \cdot \tilde{\mathbf{h}}(\vartheta) = \tilde{\mathbf{B}}(\theta,\phi)\tilde{\mathbf{h}}(\vartheta), \tag{20}$$

where "$\otimes$" denotes the Kronecker product. This implies that each element in an acoustic vector-sensor can be copied somehow via conjugate-correlation operation, thereby equivalently doubling the number of efficient elements. As in the standard MUSIC, the projection matrix $\mathbf{P}_n$ of the noise subspace can be formed by eigendecomposing $\mathbf{R}_y$. Let the $8 - Q$ eigenvectors of $\mathbf{R}_y$ according to the smallest eigenvalues be $\mathbf{v}_{Q+1}, \ldots, \mathbf{v}_8$, and denote $\mathbf{E}_n = [\mathbf{v}_{Q+1}, \ldots, \mathbf{v}_8]$. Then, $\mathbf{P}_n = \mathbf{E}_n\mathbf{E}_n^H$, and the DOAs of the sources can be obtained as

$$\begin{aligned} \theta_q, \phi_q &= \arg\min_{\theta,\phi} \mathbf{b}^H(\theta,\phi)\mathbf{P}_n\mathbf{b}(\theta,\phi) = \arg\min_{\theta,\phi} \tilde{\mathbf{h}}^H(\vartheta)\big(\tilde{\mathbf{B}}^H(\theta,\phi)\mathbf{P}_n\tilde{\mathbf{B}}(\theta,\phi)\big)\tilde{\mathbf{h}}(\vartheta) \\ &= \arg\min_{\theta,\phi} \det\big\{\tilde{\mathbf{B}}^H(\theta,\phi)\mathbf{P}_n\tilde{\mathbf{B}}(\theta,\phi)\big\}. \end{aligned} \tag{21}$$

To avoid the degeneracy problem such that $\tilde{\mathbf{B}}^H(\theta,\phi)\mathbf{P}_n\tilde{\mathbf{B}}(\theta,\phi)$ is singular for arbitrary θ and ϕ, it is required that $8 - Q \geqslant 2$ (note that $\tilde{\mathbf{B}}(\theta,\phi)$ is of size 8×2) and hence $Q \leqslant 6$. We call this method the uni-vector-sensor virtual-MUSIC, which may be easily extended to the electromagnetic analog [19] for entirely linearly polarized electromagnetic signals.

Analogous to [26], we next examine the linear independence of the virtual steering vectors to determine the number of rectilinear signals whose DOAs can be uniquely identified by virtual-MUSIC. Let $\mathbf{b}(\vartheta_1), \ldots, \mathbf{b}(\vartheta_K)$ be any K linearly dependent virtual steering vectors with distinct but arbitrary DOAs, where $\vartheta_k = [\theta_k, \phi_k]^T$. Then there must exist $3 \leqslant G \leqslant K$ linearly dependent virtual steering vectors among the above K virtual steering vectors, say, $\mathbf{b}(\vartheta_1), \ldots, \mathbf{b}(\vartheta_G)$, such that every $G-1$ vectors within them are linearly independent, i.e., $\sum_{g=1}^{G} c_g\mathbf{b}(\vartheta_g) = 0$, where $c_g \neq 0$ for $g = 1, 2, \ldots, G$. Thus,

$$\underbrace{\big[\mathbf{a}(\theta_1,\phi_1), \ldots, \mathbf{a}(\theta_G,\phi_G)\big]}_{\overset{\text{def}}{=}\mathbf{M}_l} \underbrace{\begin{bmatrix} c_1 & & & \\ & c_2 & & \\ & & \ddots & \\ & & & c_G \end{bmatrix} \begin{bmatrix} 1 & e^{-j\vartheta_1} \\ \vdots & \vdots \\ 1 & e^{-j\vartheta_G} \end{bmatrix}}_{\overset{\text{def}}{=}\mathbf{M}_r} = \mathbf{O}. \tag{22}$$

Hence, the dimension of the null space of $\mathbf{M}_l$ is at least of two since $\operatorname{rank}(\mathbf{M}_r) = 2$ for distinct ϑ. Then, $G - \operatorname{rank}(\mathbf{M}_l) \geqslant 2$ and hence $G \geqslant 2 + \operatorname{rank}(\mathbf{M}_l)$.

It was proved in [9] that *every three steering vectors* (*defined by* (1)) *corresponding to distinct DOAs are linearly independent*. Hence $\operatorname{rank}(\mathbf{M}_l) \geqslant 3$, and then $K \geqslant G \geqslant 5$. This implies that *every four virtual steering vectors with distinct DOAs are linearly independent*. Thus, given three incident signals, one could not find a new virtual steering vector, in the virtual array manifold (defined by $\mathcal{M}' = \{\mathbf{b}(\theta,\phi,\vartheta)\colon\ (\theta,\phi) \in \Theta, \vartheta \in [0, 2\pi)\}$), that intersects the

aforementioned three-dimensional signal subspace spanned by the three virtual steering vectors of the three signals. Hence, the virtual-MUSIC proposed here can process at least *three* uncorrelated noncircular sources. Note that using standard MUSIC generally only two signals can be uniquely discriminated [9]. The aperture-extension purpose thus is achieved without addition of any extra sensors in the acoustic vector-sensor.

For four signals, the corresponding steering vectors may be either linearly independent or linearly dependent. Consequently, the results established above cannot be directly used to characterize the linear independence of five virtual steering vectors for identifiability examination of four signals by the virtual-MUSIC. In Appendices A and B, we shall prove the following two propositions concerning the issue of identifying four noncircular signals with virtual-MUSIC:

Proposition 1. *The virtual-MUSIC can handle four noncircular signals that have noncoplanar propagation vectors, provided that*

$$\text{(C.1)}: \quad \operatorname{sum}([\boldsymbol{\hbar}_1, \boldsymbol{\hbar}_2, \boldsymbol{\hbar}_3]^{-1}\boldsymbol{\hbar}_4) \neq 1,$$

where $\{\boldsymbol{\hbar}_j\}_{j=1}^4$ *denotes the propagation vectors of the four signals, and "sum" signifies the sum of a vector.*

Proposition 2. *The virtual-MUSIC cannot deal with four noncircular signals satisfying either of the following two conditions*:

$$\text{(C.2)}: \quad \begin{cases} \theta_i = \theta_j = \theta, \ i \neq j; \ i, j = 1, \ldots, 4, \\ \phi_i \neq \phi_j, \ i \neq j; \ i, j = 1, \ldots, 4, \\ \phi_j = \pm\vartheta_j = \pm 2\varphi_j; \ j = 1, \ldots, 4, \end{cases}$$

$$\text{(C.3)}: \quad \begin{cases} \phi_i = \phi_j = \phi, \ i \neq j; \ i, j = 1, \ldots, 4, \\ \theta_i \neq \theta_j, \ i \neq j; \ i, j = 1, \ldots, 4, \\ \theta_j = \pm\vartheta_j = \pm 2\varphi_j; \ j = 1, \ldots, 4. \end{cases}$$

5. Colored-noise suppression

In the above, we have assumed that the sensor noise is spatially white, i.e., $E(\mathbf{n}(t)\mathbf{n}^H(t)) = \sigma_n^2\mathbf{I}$. This section, however, is devoted to colored-noise canceling which is of great practical interest for acoustic vector-sensor based DOA estimation. As is known, for example, the presence of inhomogeneous noise (noises at different elements are uncorrelated but have distinct variances) are often the case in an acoustic vector-sensor [20]. Unlike the customary methods for scalar-sensor arrays, such as those proposed in [21–25] (and references therein), the new colored-noise-immune method herein presented: (1) requires no explicit knowledge of the correlation structure of the noise; (2) does not parameterize the noise and then perform heavy joint estimation of parameters of noise and signals of interest (mostly are based on the maximum-likelihood criterion and hence of high computation complexity); (3) does not make additional assumption on the array construction such as requirements of sensor doublets and array sparsity, thereby distinguishing itself from most existing methods.

In the presence of colored-noise such that $E(\mathbf{n}(t)\mathbf{n}^H(t)) = \sigma_n^2\mathbf{R}_n$, where $\mathbf{R}_n$ is an unknown Hermitian matrix, the methods developed in Sections 3 and 4 degrade seriously in general. If the colored-noise is circular (which is often the case in many practical applications), we immediately have $E(\mathbf{n}(t)\mathbf{n}^T(t)) = \mathbf{O}$ and, hence

$$\mathbf{R}' = \frac{1}{2}\big[\mathbf{R}_{r^*} + (\mathbf{R}_{r^*})^*\big] = \mathbf{A}\frac{1}{2}\big(\mathbf{R}_{s^*} + (\mathbf{R}_{s^*})^*\big)\mathbf{A}^H = \mathbf{A}\bar{\mathbf{R}}_{s^*}\mathbf{A}^H, \tag{23}$$

where $\mathbf{R}_{r^*} = E(\mathbf{r}(t)\mathbf{r}^T(t)) = \mathbf{A}\mathbf{R}_{s^*}\mathbf{A}^H = \mathbf{A}\mathbf{R}_s\boldsymbol{\Phi}^2\mathbf{A}^H$ is the conjugate array covariance matrix, $\mathbf{r}(t)$ is defined in (2), $\mathbf{R}_{s^*} = E(\mathbf{s}(t)\mathbf{s}^T(t))$ is the conjugate source covariance matrix, and then

$$\bar{\mathbf{R}}_{s^*} = \frac{\mathbf{R}_{s^*} + (\mathbf{R}_{s^*})^*}{2} = \left(\frac{\mathbf{R}_s\boldsymbol{\Phi}^2 + \mathbf{R}_s^*\boldsymbol{\Phi}^{-2}}{2}\right) = \operatorname{Re}\big(\mathbf{R}_s\boldsymbol{\Phi}^2\big) = \big(\operatorname{Re}\big(\mathbf{R}_s\boldsymbol{\Phi}^2\big)\big)^H. \tag{24}$$

Here $\mathbf{R}'$ is Hermitian but may not be nonnegative definite. Nevertheless, thanks to the insensitivity of the conjugate correlation operation to the circular colored-noise, we have $\operatorname{rank}(\mathbf{R}') = Q$. Hence, the projection matrix $\mathbf{P}_n'$ on the noise subspace of $\mathbf{R}'$ can just be formed as the $4 - Q$ eigenvectors according to the $4 - Q$ zero eigenvalues of $\mathbf{R}'$.

(In practice, one can also take those eigenvectors that correspond to the $4-Q$ eigenvalues with the smallest magnitudes.) The MUSIC spectrum expression then can be written by

$$\theta_q, \phi_q = \arg\max_{\theta,\phi} \frac{\mathbf{a}^H(\theta,\phi)\mathbf{a}(\theta,\phi)}{\mathbf{a}^H(\theta,\phi)\mathbf{P}'_n\mathbf{a}(\theta,\phi)}. \tag{25}$$

We label this MUSIC variant as the conjugate-MUSIC. Since every *three* steering vectors in $\mathcal{M}$ with distinct DOAs are linearly independent, the conjugate-MUSIC algorithm may identify no less than two noncircular sources and is naturally blind to colored-noise.

The conjugate-MUSIC may be extended to the case of scalar-sensor array by using $\mathbf{R}_{r^*}$ or $(\mathbf{R}_{r^*})^*$ only. We also remark that the conjugate-MUSIC may deal with two perfectly correlated signals (only true for an acoustic vector-sensor). To see this, we consider two coherent signals, say, $s_1(t) = e^{j\varphi_1}s_r(t)$, $s_2(t) = \rho e^{j\varphi_2}s_r(t)$, then

$$\begin{aligned}\bar{\mathbf{R}}_{s^*} &= \frac{\mathbf{R}_{s^*} + (\mathbf{R}_{s^*})^*}{2} = \frac{1}{2}E\big(s_r^2(t)\big)\left(\begin{bmatrix} e^{j\varphi_1} \\ \rho e^{j\varphi_2}\end{bmatrix}[e^{j\varphi_1}\ \rho e^{j\varphi_2}] + \begin{bmatrix} e^{-j\varphi_1} \\ \rho e^{-j\varphi_2}\end{bmatrix}[e^{-j\varphi_1}\ \rho e^{-j\varphi_2}]\right) \\ &= \sigma_s^2\begin{bmatrix} \cos(2\varphi_1) & \rho\cos(\varphi') \\ \rho\cos(\varphi') & \rho^2\cos(2\varphi_2)\end{bmatrix},\end{aligned} \tag{26}$$

where $\varphi' = \varphi_1 + \varphi_2$. Then, $\det(\bar{\mathbf{R}}_{s^*}) = -\sigma_s^2\rho^2\sin^2\Delta\varphi$, where $\Delta\varphi = \varphi_2 - \varphi_1$. Hence, $\operatorname{rank}(\bar{\mathbf{R}}_{s^*}) = 2$ so long as $\Delta\varphi \neq k\pi$, where $k = 0, \pm1, \pm2$, which implies that the rank property of conjugate source covariance matrix can be restored by conjugately phase smoothing.

6. ESPRIT-type DOA estimator

The DOA estimators discussed in the previous sections are all based on the MUSIC method (the rooting alternatives do not appear to exist without manifold interpolation since the array manifold of an acoustic vector-sensor does not have a Vandermonde structure) which involves time consuming spectrum searching. The ESPRIT method represents another highly popular subspace-based DOA estimation method, demanding quite less computation than the MUSIC does since it is iteration-free. Moreover, ESPRIT requires no storage of manifold information [17]. To develop an ESPRIT-type DOA estimation algorithm one requires a certain shift invariance structure such as: (1) the commonly used translational invariance structure of a uniform linear array of scalar-sensors; (2) the temporally rotational invariance structure for sources having distinct frequency offsets [5]; and (3) the virtual invariance structure for non-Gaussian signals [18]. As has mentioned earlier, an acoustic vector-sensor could not offer the translational invariance. The temporal ESPRIT, on the other hand, cannot cancel the co-channel interferers. The higher order cumulant based virtual ESPRIT may deal with signals of identical frequency content. However, a well-known shortcoming of algorithms based on higher order cumulant is the high variances often exhibited by higher order statistical estimates especially in the presence of noise. In this section, a novel second-order statistics based ESPRIT variant for uni-vector-sensor DOA estimation is proposed, by incorporating noncircularity of signals and real-valued directionality offered by an acoustic vector-sensor. In this section, we only consider the case of Q uncorrelated incident signals buried in the spatially white noise.

First, we rewrite the conjugate array covariance matrix as follows (noting $\mathbf{A}$ is real-valued):

$$\mathbf{R}_{r^*} = E\big(\mathbf{r}(t)\mathbf{r}^T(t)\big) = \mathbf{A}\mathbf{R}_{s^*}\mathbf{A}^H = \mathbf{A}\mathbf{R}_s\mathbf{\Phi}^2\mathbf{A}^H. \tag{27}$$

Recall that $\mathbf{R}_r = \mathbf{A}\mathbf{R}_s\mathbf{A}^H + \sigma_n^2\mathbf{I}$, then, provided that the noise variance is known or could be estimated somehow, we may obtain the cleaned array covariance matrix as $\breve{\mathbf{R}}_r \overset{\text{def}}{=} \mathbf{R}_r - \sigma_n^2\mathbf{I} = \mathbf{A}\mathbf{R}_s\mathbf{A}^H$. As a consequence, the ESPRIT matrix pencil required by the ESPRIT algorithm may be formed as $\{\breve{\mathbf{R}}_r, (\mathbf{R}_{r^*})^H\}$.

From the structure of $\{\breve{\mathbf{R}}_r, (\mathbf{R}_{r^*})^H\}$, there must exist a 4×4 matrix $\mathbf{\Psi}$, such that $\mathbf{\Psi}\breve{\mathbf{R}}_r = (\mathbf{R}_{r^*})^H$. However, system of equation $\mathbf{\Psi}\breve{\mathbf{R}}_r = (\mathbf{R}_{r^*})^H$ is underdetermined since $\operatorname{rank}(\breve{\mathbf{R}}_r) = Q < 4$.

To deal with the above nonuniqueness problem, we propose to solve the next problem:

$$\kappa\|\mathbf{\Psi}'\|_F^2 + \big\|\big(\breve{\mathbf{R}}_r\big)^H\mathbf{\Psi}' - \mathbf{R}_{r^*}\big\|_F^2,$$

which is a norm-penalized scheme and amounts to solving the next linear least squares fitting:

$$\arg\min_{\boldsymbol{\Psi}} \left\| \begin{pmatrix} \sqrt{\kappa}\,\mathbf{I}_{4,4} \\ (\breve{\mathbf{R}}_r)^H \end{pmatrix} \boldsymbol{\Psi}' - \begin{pmatrix} \mathbf{O}_{4,4} \\ \mathbf{R}_{r^*} \end{pmatrix} \right\|_F^2, \tag{28}$$

where κ is the regularization parameter. The solution to (28) is $\boldsymbol{\Psi}'(\kappa) = (\kappa\mathbf{I} + \breve{\mathbf{R}}_r \breve{\mathbf{R}}_r^H)^{-1} \breve{\mathbf{R}}_r \mathbf{R}_{r^*}$. We next express $\breve{\mathbf{R}}_r$ in terms of its eigen-decomposition, that is,

$$\breve{\mathbf{R}}_r = \mathbf{U}_s \boldsymbol{\Sigma}_s \mathbf{U}_s^H + \mathbf{U}_n \boldsymbol{\Sigma}_n \mathbf{U}_n^H = \mathbf{U}\boldsymbol{\Sigma}\mathbf{U}^H, \tag{29}$$

where $\mathbf{U}_s\mathbf{U}_s^H + \mathbf{U}_n\mathbf{U}_n^H = \mathbf{I}_{4,4}$ and $\mathbf{U}_s^H\mathbf{U}_s = \mathbf{I}_{Q,Q}$, $\mathbf{U}_s^H\mathbf{U}_n = \mathbf{O}$, and

$$\begin{cases} \boldsymbol{\Sigma}_s = \operatorname{diag}(\upsilon_1, \upsilon_2, \ldots, \upsilon_Q), \\ \boldsymbol{\Sigma}_n = \operatorname{diag}(0, 0, \ldots, 0), \end{cases} \tag{30}$$

in which $\upsilon_1, \ldots, \upsilon_Q$ are Q non-zero real eigenvalues of $\breve{\mathbf{R}}_r$. Then,

$$\begin{aligned} \boldsymbol{\Psi}'(\kappa) &= \left(\kappa\mathbf{I} + \breve{\mathbf{R}}_r \breve{\mathbf{R}}_r^H\right)^{-1} \breve{\mathbf{R}}_r \mathbf{R}_{r^*} = \left(\kappa\mathbf{I} + \mathbf{U}\boldsymbol{\Sigma}^2\mathbf{U}^H\right)^{-1} \mathbf{U}\boldsymbol{\Sigma}\mathbf{U}^H\mathbf{R}_{r^*} = \mathbf{U}\left(\kappa\mathbf{I} + \boldsymbol{\Sigma}^2\right)^{-1}\boldsymbol{\Sigma}\mathbf{U}^H\mathbf{R}_{r^*} \\ &= \mathbf{U}_s \operatorname{diag}\left(\frac{\upsilon_1}{\upsilon_1^2 + \kappa}, \ldots, \frac{\upsilon_Q}{\upsilon_Q^2 + \kappa}\right)\mathbf{U}_s^H\mathbf{R}_{r^*}. \end{aligned} \tag{31}$$

Therefore, $(\boldsymbol{\Psi}')^H|_{\kappa\to 0} = \mathbf{A}\boldsymbol{\Phi}^{-2}\mathbf{A}^+$, by noting that $\mathbf{R}_s\mathbf{A}^H = \mathbf{A}^+\mathbf{U}_s\boldsymbol{\Sigma}_s\mathbf{U}_s^H$, where $\mathbf{A}^+ = (\mathbf{A}^H\mathbf{A})^{-1}\mathbf{A}^H$. In fact, $(\boldsymbol{\Psi}')^H$ is the minimum Frobenius-norm solution to $\boldsymbol{\Psi}\breve{\mathbf{R}}_r = (\mathbf{R}_{r^*})^H$. (In practice, $\breve{\mathbf{R}}_r$ can only be estimated from finite noisy data samples. The estimate $\widehat{\mathbf{R}}_r$ becomes full rank but may have very large condition number, and the solution to (28) becomes $\widehat{\mathbf{R}}_r^{-1}\widehat{\mathbf{R}}_{r^*}$, where $\widehat{\mathbf{R}}_{r^*}$ is the estimate of $\mathbf{R}_{r^*}$. To enhance numerical stability, we suggest to truncate $\widehat{\mathbf{R}}_r$ prior to performing ESPRIT. That is, $\widehat{\mathbf{R}}_r = \widehat{\mathbf{U}}_s\widehat{\boldsymbol{\Sigma}}_s\widehat{\mathbf{U}}_s^H$, where $\widehat{\mathbf{U}}_s$ and $\widehat{\boldsymbol{\Sigma}}_s$ are the estimates of $\mathbf{U}_s$ and $\boldsymbol{\Sigma}_s$, respectively.) $(\boldsymbol{\Psi}')^H$ is of rank Q and has Q dominant eigenvectors $\boldsymbol{\epsilon}_q$ equal to $\xi_q\mathbf{a}_q$, where $q = 1, 2, \ldots, Q$, and ξ_q is an unknown scalar, since $(\boldsymbol{\Psi}')^H\mathbf{A} = \mathbf{A}\boldsymbol{\Phi}^{-2}$. Thus, the Q propagation vectors $\boldsymbol{\eta}_q$ (and hence the Q DOAs) of the Q incident signals can be obtained as

$$\boldsymbol{\eta}_q = \frac{\boldsymbol{\epsilon}_q(1{:}3)}{\boldsymbol{\epsilon}_q(4)}, \quad q = 1, 2, \ldots, Q. \tag{32}$$

We name the above single-vector-sensor ESPRIT the noncircular-ESPRIT. This new ESPRIT variant removes the requirement in the uni-vector-sensor temporal ESPRIT that the signals must have different frequencies [5]. Moreover, the noncircular-ESPRIT excels the cumulant ESPRIT [18] in lower estimation variance and the capability of non-Gaussian noise suppression. The noncircular ESPRIT, however, dose not apply to an array of scalar-sensors because $\mathbf{A} \neq \mathbf{A}^*$ in that a case.

7. Simulation results and discussions

In this section, some simulation results are provided to illustrate the noncircular methods proposed above. We first examine the behavior of the phase smoothing technique. The signals used are two unipower coherent BPSK signals. The initial phases are $\varphi_1 = \pi/7$, $\varphi_2 = \pi/3$, and $\rho = 1$. The two DOAs are (30°, 90°), (120°, 90°), respectively. The additive noise is temporally and spatially white. The number of snapshots is 200, and the signal-to-noise ratio (SNR) is 10 dB. The results shown in Fig. 2 are the azimuth-only spectrums for the standard MUSIC without any preprocessing procedure, the direct phase smoothing based MUSIC, and the squared phase smoothing based MUSIC, respectively. It is seen that both of the two phase smoothing techniques can decorrelate the signals successfully. We further compare the direct phase smoothing and squared phase smoothing in terms of RMSE (*root mean squared error*) which is defined as $\sqrt{E[(\hat{\theta} - \theta)^2]}$, where θ and $\hat{\theta}$ denote the true and estimated DOAs, respectively. The statistics shown are computed by averaging results of 200 independent trails. Results displayed in Figs. 3 and 4 suggest that the squared phase smoothing is superior to the direct phase smoothing especially in the difficult scenarios (i.e., low SNR and short data length).

We next investigate the virtual-MUSIC method. We first consider three uncorrelated signals from azimuths 8°, 150°, and 250°, respectively. The elevations of them are all of 90°. The initial phase of the three signals are of $\pi/7, \pi/3$, and $\pi/6$, respectively. The noise is temporally and spatially white. The SNR is 30 dB whereas the number

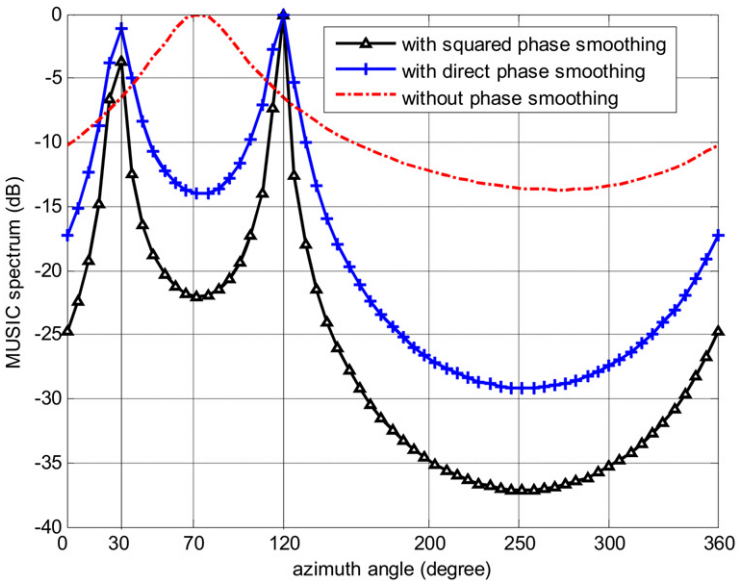

Fig. 2. Azimuth-only MUSIC spectrums with and without phase smoothing for two coherent BPSK signals.

of snapshot is 300. The curves plotted in Fig. 5 are the azimuth-only spectrum of virtual-MUSIC and standard MUSIC. As expected, the virtual-MUSIC can uniquely resolve the three signals whereas the standard MUSIC could not. We further consider four signals from $(80°, 30°)$, $(150°, 120°)$, $(250°, 60°)$, and $(300°, 150°)$, with initial phases $2\pi/9, 5\pi/12, 25\pi/36$, and $5\pi/6$, respectively. It can be checked that these four signals satisfy condition (C.1). It is observed in Fig. 6 the identifiability of the four signals. We proceed to consider four signals that obey condition (C.2). The azimuth angles are 80°, 150°, 250°, and 300°, respectively. The elevations are all set to be 90°. The initial phases are $40\pi/180, 75\pi/180, 125\pi/180$, and $150\pi/180$, respectively. The corresponding azimuth-only spectrum is shown in Fig. 7. As expected, the virtual MUSIC fails. The result given in Fig. 8 is for four signals from the same direction but with distinct initial phases ($\pi/7, \pi/3, \pi/6$, and $\pi/4$). Clearly, these four signals have linearly dependent steering vectors; however, it is seen that they can still be uniquely distinguished by the virtual-MUSIC. This example suggests that it would be wrong to claim that *every five virtual steering vectors are linearly dependent if* $\boldsymbol{\mathcal{A}}^{(4)}$ is rank deficient. In any case, the completely tight characterization of five virtual steering vectors associated with arbitrarily distinct DOAs remains unresolved.

We next compare the noncircular-ESPRIT with the customary cum-ESPRIT in [18]. We plot the overall root MSAE (*mean squared angular error*[1]) defined as $\sqrt{\sum_{q=1}^{Q} E[(\cos^{-1}(\hat{\boldsymbol{\hbar}}_q^T \boldsymbol{\hbar}_q))^2]}$, wherein $\boldsymbol{\hbar}_q$ and $\hat{\boldsymbol{\hbar}}_q$ are the qth true and estimated signal propagation vectors, respectively. All the statistics shown in the figures are computed by averaging results of 200 independent trials. Two uncorrelated signals from $(145°, 30°)$ and $(30°, 60°)$ with initial phases 0 and $\pi/3$, respectively, are considered in the simulations. The number of snapshot is fixed as 50 when SNR is varied. The SNR is 10 dB when the snapshot number is varied. The results plotted in Figs. 9 and 10 are the comparison of $\sqrt{\text{MSAE}}$ curves against SNR and the number of snapshot, respectively. It is visibly seen that the noncircular ESPRIT outperforms the cum-ESPRIT significantly with respect to both estimation variance and convergence speed.

We finally examine the colored-noise suppression capability of the conjugate MUSIC. We consider two uncorrelated signals from azimuths 30° and 120° (both from elevation 90°). The initial phases of the signals are of $\pi/14$ and $\pi/6$, respectively. The temporally-white noise is spatially correlated with the next covariance matrix:

[1] The term "MSAE" was coined by Nehorai in [1] which can serve as a useful performance metric for azimuth-elevation 2D DOA estimation in the whole 3D space. Let (θ, ϕ) and $(\hat{\theta}, \hat{\phi})$ respectively be the true and estimated azimuth and elevation angles while $\boldsymbol{\hbar} = [-\cos\theta\sin\phi, \sin\theta\sin\phi, \cos\phi]^T$ and $\hat{\boldsymbol{\hbar}} = [-\cos\hat{\theta}\sin\hat{\phi}, \sin\hat{\theta}\sin\hat{\phi}, \cos\hat{\phi}]^T$ be the corresponding propagation vectors, and δ be the angular error between $\boldsymbol{\hbar}$ and $\hat{\boldsymbol{\hbar}}$, the MSAE measure then is defined as $E[\delta^2] = E[(\cos^{-1}(\hat{\boldsymbol{\hbar}}^T \boldsymbol{\hbar}))^2]$. From the definition, a lower MSAE implies a better 2D DOA estimate.

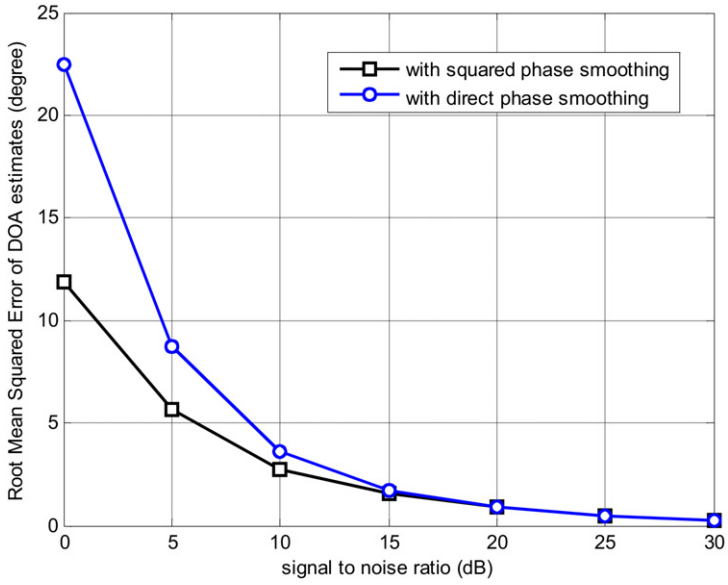

(a)

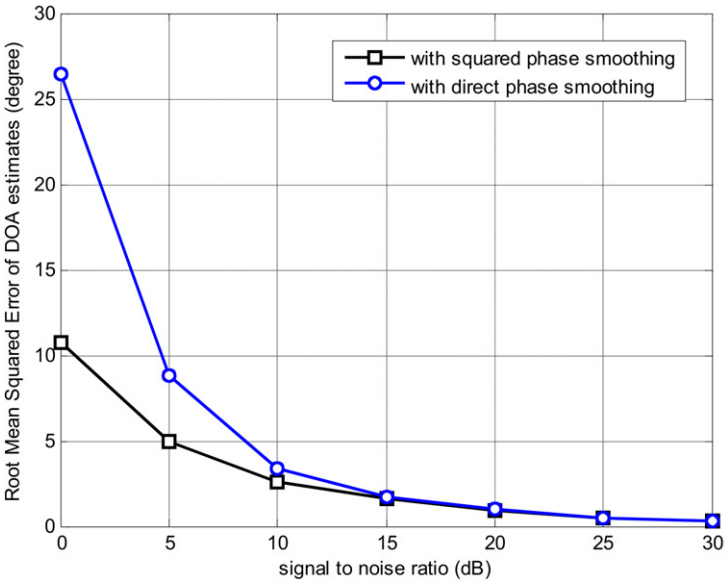

(b)

Fig. 3. RMSE curve of phase smoothing based DOA estimates, against SNR. RMSE vs SNR curve for the signal from (a) 30° and (b) 120°.

$$\sigma_n^2\mathbf{R}_n = \sigma_n^2\begin{bmatrix} 1 & 0.3080+j0.1276 & 0.2887+j0.1667 & 0.2357+j0.2357 \\ 0.3080-j0.1276 & 1 & 0.3080+j0.1276 & 0.2887+j0.1667 \\ 0.2887-j0.1667 & 0.3080-j0.1276 & 1 & 0.3080+j0.1276 \\ 0.2357-j0.2357 & 0.2887-j0.1667 & 0.3080-j0.1276 & 1 \end{bmatrix}.$$

The SNR (defined as $10\log\sigma_n^{-2}$ for unipower signals) is 0 dB whereas the number of snapshot is 5000. Results in Fig. 11 show that the proposed conjugate-MUSIC works well in the presence of colored-noise while the standard MUSIC almost fails in such a case. The curve shown in Fig. 12, however, is for two coherent signals from the same directions with initial phases $\pi/14$ and $9\pi/28$. For comparison, the curve for two uncorrelated signals is also included in the plot. Visibly, the two signals are clearly discriminated by the conjugate MUSIC regardless of coherence. The results shown in Figs. 13 and 14 are the 2D spectrums of conjugate MUSIC for two uncorrelated and coherent signals,

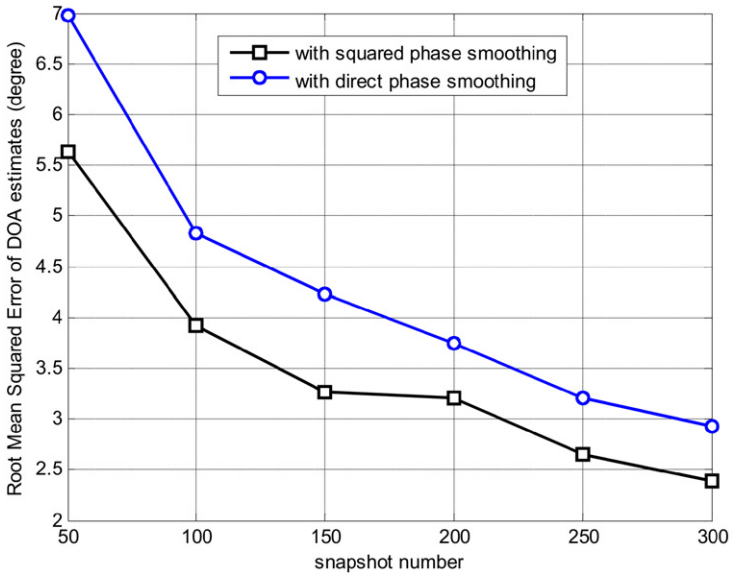

(a)

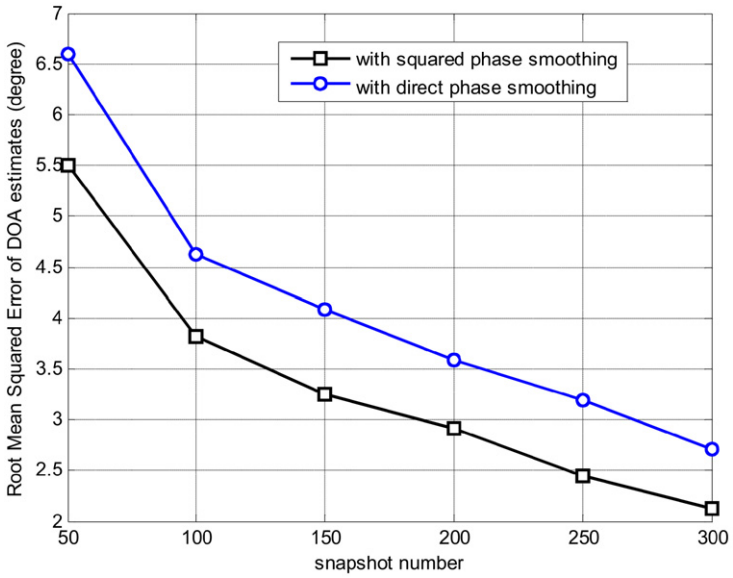

(b)

Fig. 4. RMSE curve of phase smoothing based DOA estimates, against snapshot number. RMSE vs snapshot curve for the signal from (a) 30° and (b) 120°.

respectively. The DOAs for both cases are of $(30°, 30°)$, $(200°, 120°)$. The initial phases are still $\pi/14$ and $9\pi/28$. Again, the blindness of the conjugate MUSIC to the colored noise is apparently observed.

Appendix A. Proof of Proposition 1

In this appendix, we give the proof of Proposition 1. Let L denote an integer, and

$$\mathcal{A}^{(L)} = \begin{bmatrix} 1 & 1 & \dots & 1 \\ \cos\theta_1 \sin\phi_1 & \cos\theta_2 \sin\phi_2 & \dots & \cos\theta_L \sin\phi_L \\ \sin\theta_1 \sin\phi_1 & \sin\theta_2 \sin\phi_2 & \dots & \sin\theta_L \sin\phi_L \\ \cos\phi_1 & \cos\phi_2 & \dots & \cos\phi_L \end{bmatrix} = \big[\mathbf{a}(\theta_1, \phi_1), \dots, \mathbf{a}(\theta_L, \phi_L)\big], \tag{A.1}$$

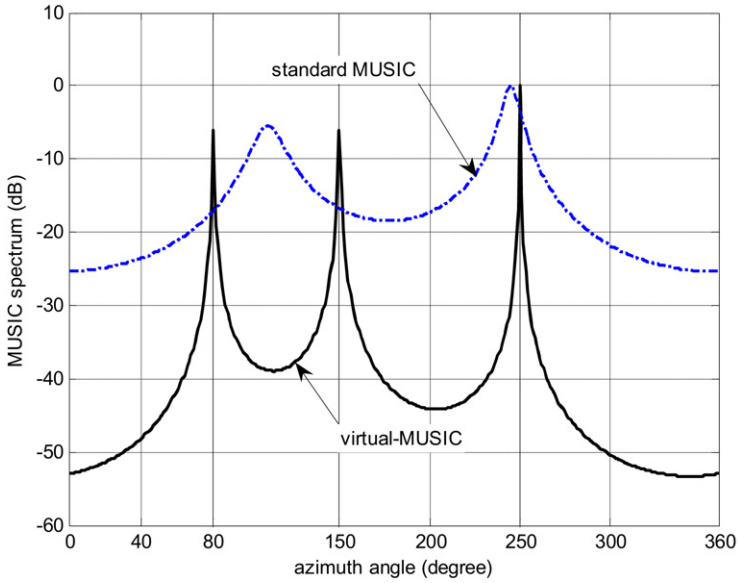

Fig. 5. Azimuth-only standard and virtual MUSIC spectrums for three uncorrelated BPSK signals.

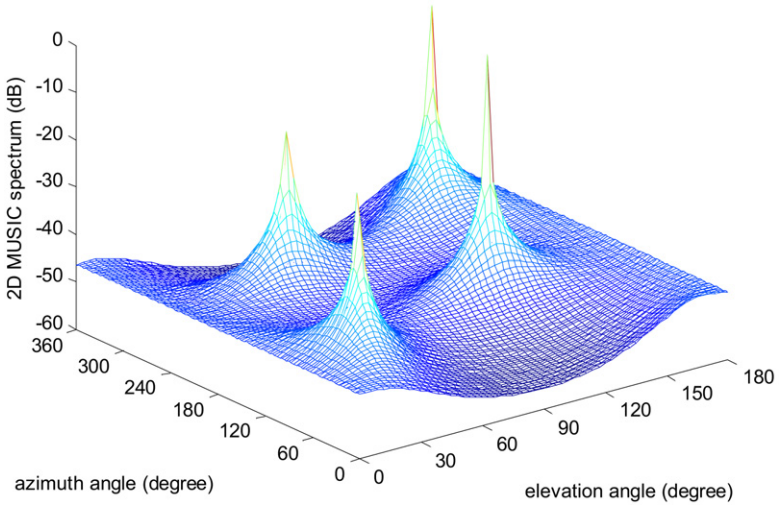

Fig. 6. Virtual-MUSIC 2D spectrum for four uncorrelated BPSK signals satisfying condition (C.1).

$$\mathcal{B}^{(L)} = \begin{bmatrix} 1 & 1 & \dots & 1 \\ \cos\theta_1 \sin\phi_1 & \cos\theta_2 \sin\phi_2 & \dots & \cos\theta_L \sin\phi_L \\ \sin\theta_1 \sin\phi_1 & \sin\theta_2 \sin\phi_2 & \dots & \sin\theta_L \sin\phi_L \\ \cos\phi_1 & \cos\phi_2 & \dots & \cos\phi_L \\ e^{-j\vartheta_1} & e^{-j\vartheta_2} & \dots & e^{-j\vartheta_L} \\ e^{-j\vartheta_1}\cos\theta_1 \sin\phi_1 & e^{-j\vartheta_2}\cos\theta_2 \sin\phi_2 & \dots & e^{-j\vartheta_L}\cos\theta_L \sin\phi_L \\ e^{-j\vartheta_1}\sin\theta_1 \sin\phi_1 & e^{-j\vartheta_2}\sin\theta_2 \sin\phi_2 & \dots & e^{-j\vartheta_L}\sin\theta_L \sin\phi_L \\ e^{-j\vartheta_1}\cos\phi_1 & e^{-j\vartheta_2}\cos\phi_2 & \dots & e^{-j\vartheta_L}\cos\phi_L \end{bmatrix}$$

$$= \big[\mathbf{b}(\theta_1, \phi_1), \dots, \mathbf{b}(\theta_L, \phi_L)\big] = \begin{bmatrix} \mathcal{A}^{(L)} \\ \mathcal{A}^{(L)}[\mathcal{Q}^{(L)}]^{-1} \end{bmatrix}, \tag{A.2}$$

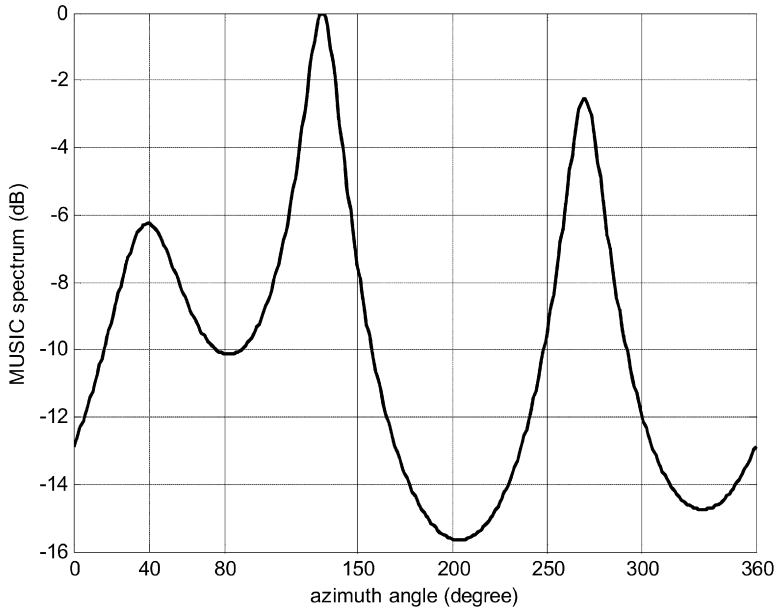

Fig. 7. Azimuth-only virtual-MUSIC spectrum for four uncorrelated BPSK signals satisfying condition (C.2).

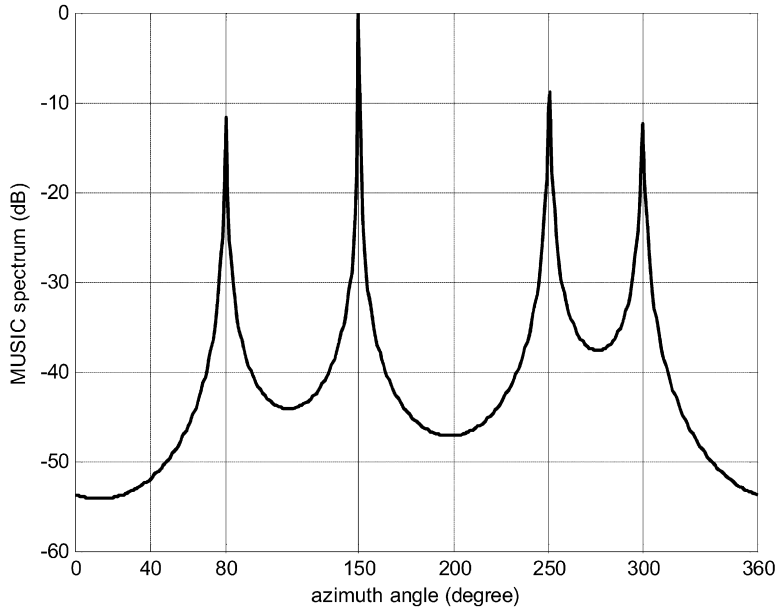

Fig. 8. Azimuth-only virtual-MUSIC spectrum for four uncorrelated BPSK signals with $\operatorname{rank}(\boldsymbol{\mathcal{A}}^{(4)}) < 4$.

where $\boldsymbol{\mathcal{Q}}^{(L)} = \operatorname{diag}(e^{j\vartheta_1}, \ldots, e^{j\vartheta_L})$. For $L = 4$, $\boldsymbol{\mathcal{A}}^{(4)}$ may be either full rank or rank deficient. For example, it can be verified that four steering vectors associated with either identical azimuth angle or identical elevation angle are linearly dependent. That is,

$$\operatorname{rank}\bigl(\boldsymbol{\mathcal{A}}^{(4)}\bigr) = \operatorname{rank}\begin{bmatrix} 1 & 1 & 1 & 1 \\ \cos\theta_1 \sin\phi & \cos\theta_2 \sin\phi & \cos\theta_3 \sin\phi & \cos\theta_4 \sin\phi \\ \sin\theta_1 \sin\phi & \sin\theta_2 \sin\phi & \sin\theta_3 \sin\phi & \sin\theta_4 \sin\phi \\ \cos\phi & \cos\phi & \cos\phi & \cos\phi \end{bmatrix} = 3, \tag{A.3}$$

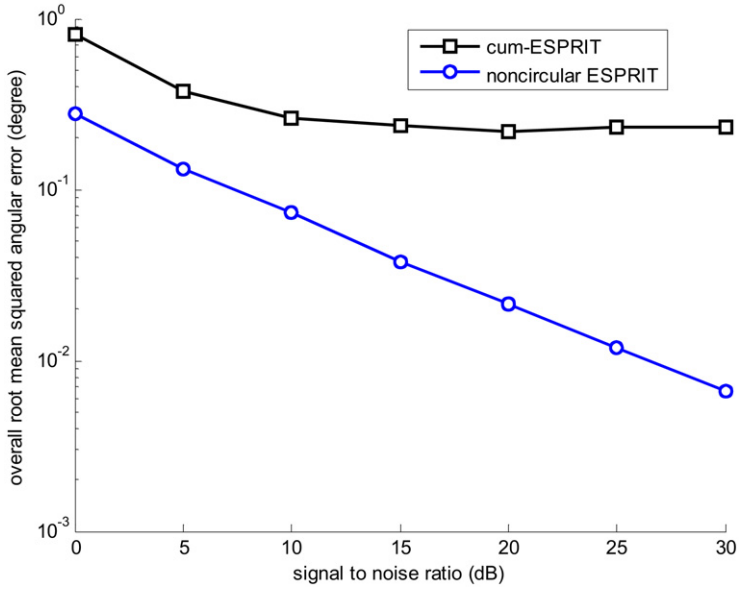

Fig. 9. Overall root MSAE comparison of noncircular ESPRIT and cum-ESPRIT against SNR.

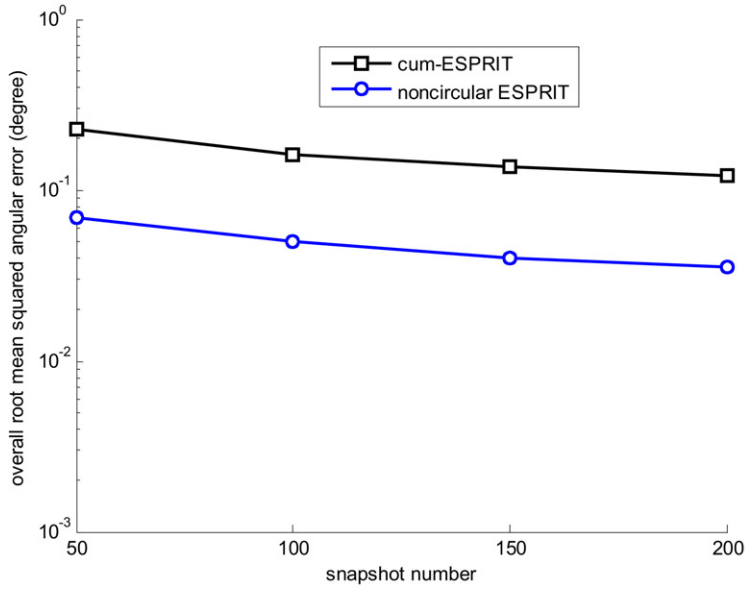

Fig. 10. Overall root MSAE comparison of noncircular ESPRIT and cum-ESPRIT against number of snapshot.

$$\operatorname{rank}\left(\boldsymbol{\mathcal{A}}^{(4)}\right) = \operatorname{rank}\begin{bmatrix} 1 & 1 & 1 & 1 \\ \cos\theta\sin\phi_1 & \cos\theta\sin\phi_2 & \cos\theta\sin\phi_3 & \cos\theta\sin\phi_4 \\ \sin\theta\sin\phi_1 & \sin\theta\sin\phi_2 & \sin\theta\sin\phi_3 & \sin\theta\sin\phi_4 \\ \cos\phi_1 & \cos\phi_2 & \cos\phi_3 & \cos\phi_4 \end{bmatrix} = 3. \tag{A.4}$$

We proceed to prove a sufficient condition under which $\operatorname{rank}(\boldsymbol{\mathcal{A}}^{(4)}) = 4$ and hence $\operatorname{rank}(\boldsymbol{\mathcal{B}}^{(5)}) = 5$. Consider four signals that have noncoplanar propagation vectors $\{\boldsymbol{\hbar}_j\}_{j=1}^{4}$, and satisfy condition (C.1), i.e., $\operatorname{sum}([\boldsymbol{\hbar}_1, \boldsymbol{\hbar}_2, \boldsymbol{\hbar}_3]^{-1}\boldsymbol{\hbar}_4) \neq 1$. Then, $\operatorname{rank}(\boldsymbol{\mathcal{A}}^{(4)}) = 4$, and, from the discussions in Section 4, there does not exist in the virtual array manifold a different virtual steering vector that is dependent on these four virtual steering vectors. To prove this, we first note that

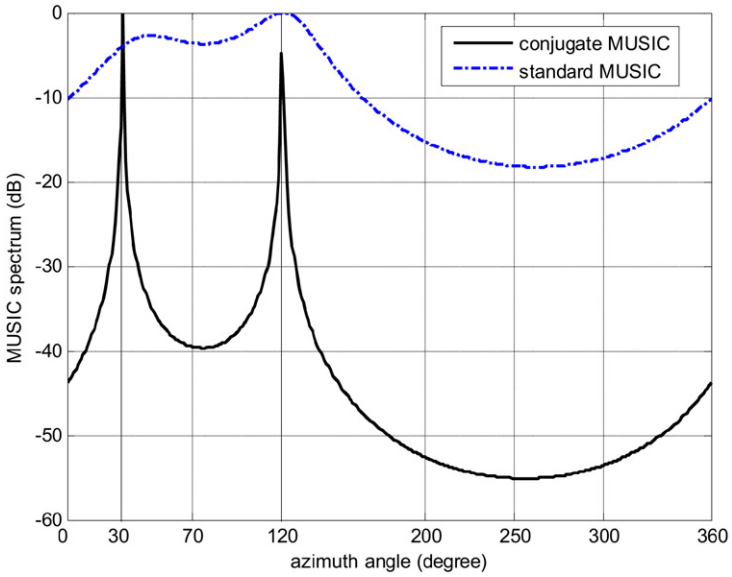

Fig. 11. Spectrums of conjugate MUSIC and standard MUSIC for two uncorrelated signals buried in colored noise.

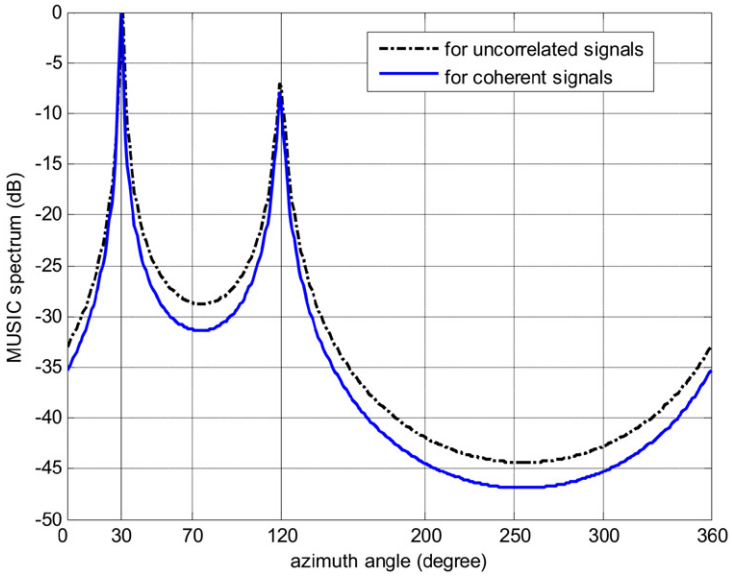

Fig. 12. Spectrums of conjugate MUSIC for two uncorrelated and coherent signals buried in colored noise.

$$\begin{aligned}\operatorname{rank}\bigl(\mathcal{A}^{(4)}\bigr) &= \operatorname{rank}\begin{bmatrix} 1 & 1 & 1 & 1 \\ \cos\theta_1\sin\phi_1 & \cos\theta_2\sin\phi_2 & \cos\theta_3\sin\phi_3 & \cos\theta_4\sin\phi_4 \\ \sin\theta_1\sin\phi_1 & \sin\theta_2\sin\phi_2 & \sin\theta_3\sin\phi_3 & \sin\theta_4\sin\phi_4 \\ \cos\phi_1 & \cos\phi_2 & \cos\phi_3 & \cos\phi_4 \end{bmatrix} \\ &= \operatorname{rank}\begin{bmatrix} 1 & 1 & 1 & 1 \\ \hbar_1 & \hbar_2 & \hbar_3 & \hbar_4 \end{bmatrix} = \operatorname{rank}\begin{bmatrix} \hbar_1 & \hbar_2 & \hbar_3 & \hbar_4 \\ 1 & 1 & 1 & 1 \end{bmatrix} = \operatorname{rank}\begin{bmatrix} \boldsymbol{\Delta}_1 & \hbar_4 \\ \boldsymbol{\Delta}_2^T & 1 \end{bmatrix}, \end{aligned} \tag{A.5}$$

where $\boldsymbol{\Delta}_1 = [\hbar_1, \hbar_2, \hbar_3]$, $\boldsymbol{\Delta}_2 = [1, 1, 1]^T$. Geometrically, if $\hbar_1, \hbar_2, \hbar_3$ are not coplanar, we must have $\operatorname{rank}(\boldsymbol{\Delta}_1) = 3$. Then,

$$\begin{bmatrix} \mathbf{I}_3 & 0 \\ -\boldsymbol{\Delta}_2^T\boldsymbol{\Delta}_1^{-1} & 1 \end{bmatrix}\begin{bmatrix} \boldsymbol{\Delta}_1 & \hbar_4 \\ \boldsymbol{\Delta}_2^T & 1 \end{bmatrix} = \begin{bmatrix} \boldsymbol{\Delta}_1 & \hbar_4 \\ 0 & 1 - \boldsymbol{\Delta}_2^T\boldsymbol{\Delta}_1^{-1}\hbar_4 \end{bmatrix}. \tag{A.6}$$

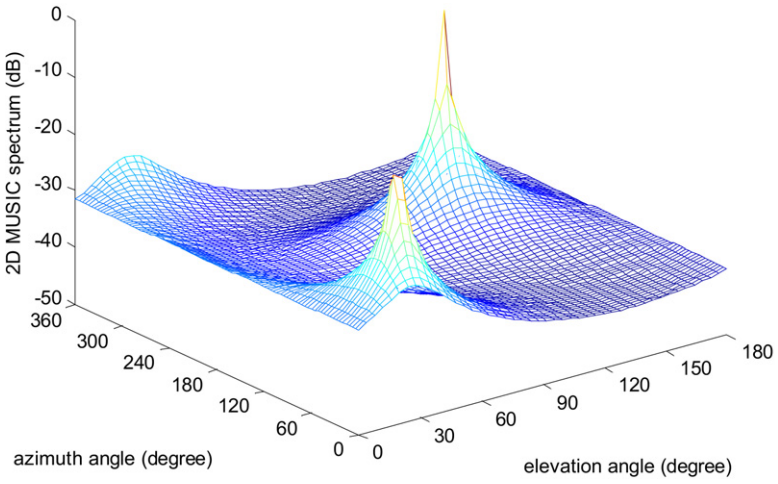

Fig. 13. Conjugate MUSIC 2D spectrum for two uncorrelated signals.

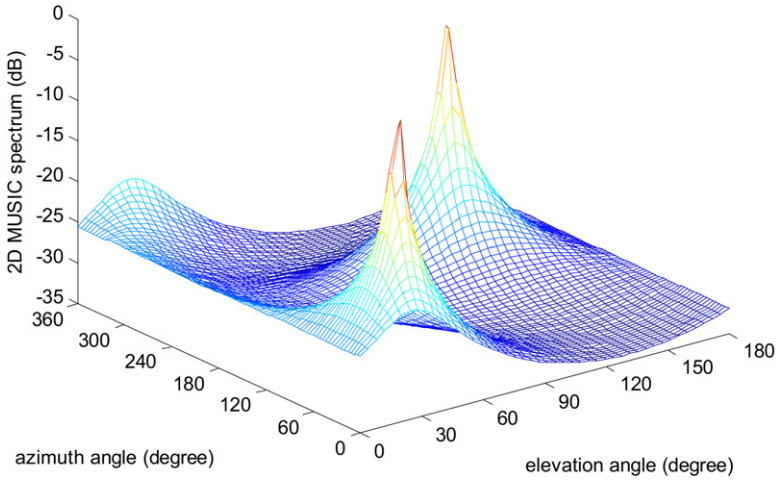

Fig. 14. Conjugate MUSIC 2D spectrum for two coherent signals.

Consequently,

$$\det\begin{bmatrix} \mathbf{I}_3 & 0 \\ -\boldsymbol{\Delta}_2^T\boldsymbol{\Delta}_1^{-1} & 1 \end{bmatrix}\begin{bmatrix} \boldsymbol{\Delta}_1 & \boldsymbol{\hbar}_4 \\ \boldsymbol{\Delta}_2^T & 1 \end{bmatrix} = \det\begin{bmatrix} \boldsymbol{\Delta}_1 & \boldsymbol{\hbar}_4 \\ \boldsymbol{\Delta}_2^T & 1 \end{bmatrix} = \det\begin{bmatrix} \boldsymbol{\Delta}_1 & \boldsymbol{\hbar}_4 \\ 0 & 1-\boldsymbol{\Delta}_2^T\boldsymbol{\Delta}_1^{-1}\boldsymbol{\hbar}_4 \end{bmatrix}$$
$$= \det(\boldsymbol{\Delta}_1)\det\bigl(1-\boldsymbol{\Delta}_2^T\boldsymbol{\Delta}_1^{-1}\boldsymbol{\hbar}_4\bigr) = \bigl(1-\boldsymbol{\Delta}_2^T\boldsymbol{\Delta}_1^{-1}\boldsymbol{\hbar}_4\bigr)\det(\boldsymbol{\Delta}_1). \tag{A.7}$$

Since $\det(\boldsymbol{\Delta}_1)\neq 0, \operatorname{rank}(\boldsymbol{\mathcal{A}}^{(4)}) = 4$ given that $1-\boldsymbol{\Delta}_2^T\boldsymbol{\Delta}_1^{-1}\boldsymbol{\hbar}_4 = 1-\operatorname{sum}(\boldsymbol{\Delta}_1^{-1}\boldsymbol{\hbar}_4)\neq 0$. We thus conclude that every five virtual steering vectors associated with distinct DOAs are linearly independent if four of the five signals have noncoplanar propagation vectors and condition (C.1) holds true. According to this observation, virtual MUSIC can accommodate four signals that have noncoplanar propagation vectors and satisfy condition (C.1).

Appendix B. Proof of Proposition 2

To prove Proposition 2, we need to show that if five signals satisfy either of conditions (C.2) and (C.3), the corresponding five virtual steering vectors are linearly dependent. Let us write

$$\boldsymbol{\mathcal{B}}^{(5)} = \begin{bmatrix} 1 & 1 & 1 & 1 & 1 \\ \cos\theta\sin\phi_1 & \cos\theta\sin\phi_2 & \cos\theta\sin\phi_3 & \cos\theta\sin\phi_4 & \cos\theta\sin\phi_5 \\ \sin\theta\sin\phi_1 & \sin\theta\sin\phi_2 & \sin\theta\sin\phi_3 & \sin\theta\sin\phi_4 & \sin\theta\sin\phi_5 \\ \cos\phi_1 & \cos\phi_2 & \cos\phi_3 & \cos\phi_4 & \cos\phi_5 \\ e^{\pm j\phi_1} & e^{\pm j\phi_2} & e^{\pm j\phi_3} & e^{\pm j\phi_4} & e^{\pm j\phi_5} \\ e^{\pm j\phi_1}\cos\theta\sin\phi_1 & e^{\pm j\phi_2}\cos\theta\sin\phi_2 & e^{\pm j\phi_3}\cos\theta\sin\phi_3 & e^{\pm j\phi_4}\cos\theta\sin\phi_4 & e^{\pm j\phi_5}\cos\theta\sin\phi_5 \\ e^{\pm j\phi_1}\sin\theta\sin\phi_1 & e^{\pm j\phi_2}\sin\theta\sin\phi_2 & e^{\pm j\phi_3}\sin\theta\sin\phi_3 & e^{\pm j\phi_4}\sin\theta\sin\phi_4 & e^{\pm j\phi_5}\sin\theta\sin\phi_5 \\ e^{\pm j\phi_1}\cos\phi_1 & e^{\pm j\phi_2}\cos\phi_2 & e^{\pm j\phi_3}\cos\phi_3 & e^{\pm j\phi_4}\cos\phi_4 & e^{\pm j\phi_5}\cos\phi_5 \end{bmatrix}. \tag{B.1}$$

And note that

$$\begin{aligned} &\operatorname{rank}\begin{bmatrix} e^{-j\phi_1} & e^{-j\phi_2} & e^{-j\phi_3} & e^{-j\phi_4} \\ 1 & 1 & 1 & 1 \\ e^{j\phi_1} & e^{j\phi_2} & e^{j\phi_3} & e^{j\phi_4} \\ e^{j2\phi_1} & e^{j2\phi_2} & e^{j2\phi_3} & e^{j2\phi_4} \end{bmatrix} \\ &\quad= \operatorname{rank}\left(\begin{bmatrix} 1 & 1 & 1 & 1 \\ e^{j\phi_1} & e^{j\phi_2} & e^{j\phi_3} & e^{j\phi_4} \\ e^{j2\phi_1} & e^{j2\phi_2} & e^{j2\phi_3} & e^{j2\phi_4} \\ e^{j3\phi_1} & e^{j3\phi_2} & e^{j3\phi_3} & e^{j3\phi_4} \end{bmatrix} \underbrace{\begin{bmatrix} e^{-j\phi_1} & & & \\ & e^{-j\phi_2} & & \\ & & e^{-j\phi_3} & \\ & & & e^{-j\phi_4} \end{bmatrix}}_{\triangleq\boldsymbol{\Upsilon}} \right) \\ &\quad\overset{\operatorname{rank}(\boldsymbol{\Upsilon})=4}{=} \operatorname{rank}\begin{bmatrix} 1 & 1 & 1 & 1 \\ e^{j\phi_1} & e^{j\phi_2} & e^{j\phi_3} & e^{j\phi_4} \\ e^{j2\phi_1} & e^{j2\phi_2} & e^{j2\phi_3} & e^{j2\phi_4} \\ e^{j3\phi_1} & e^{j3\phi_2} & e^{j3\phi_3} & e^{j3\phi_4} \end{bmatrix} = 4 \end{aligned}$$

and

$$\begin{aligned} \operatorname{rank}\begin{bmatrix} e^{-j\phi_1} & e^{-j\phi_2} & e^{-j\phi_3} & e^{-j\phi_4} \\ 1 & 1 & 1 & 1 \\ e^{j\phi_1} & e^{j\phi_2} & e^{j\phi_3} & e^{j\phi_4} \\ e^{-j2\phi_1} & e^{-j2\phi_2} & e^{-j2\phi_3} & e^{-j2\phi_4} \end{bmatrix} &= \operatorname{rank}\begin{bmatrix} e^{-j2\phi_1} & e^{-j2\phi_2} & e^{-j2\phi_3} & e^{-j2\phi_4} \\ e^{-j\phi_1} & e^{-j\phi_2} & e^{-j\phi_3} & e^{-j\phi_4} \\ 1 & 1 & 1 & 1 \\ e^{j\phi_1} & e^{j\phi_2} & e^{j\phi_3} & e^{j\phi_4} \end{bmatrix} \\ &= \operatorname{rank}\left(\begin{bmatrix} 1 & 1 & 1 & 1 \\ e^{j\phi_1} & e^{j\phi_2} & e^{j\phi_3} & e^{j\phi_4} \\ e^{j2\phi_1} & e^{j2\phi_2} & e^{j2\phi_3} & e^{j2\phi_4} \\ e^{j3\phi_1} & e^{j3\phi_2} & e^{j3\phi_3} & e^{j3\phi_4} \end{bmatrix} \boldsymbol{\Upsilon}^2 \right) = 4. \end{aligned}$$

Hence, there must exist a 4×1 vector $\mathbf{y}^{(4)}$ such that

$$\begin{bmatrix} e^{-j\phi_1} & e^{-j\phi_2} & e^{-j\phi_3} & e^{-j\phi_4} \\ 1 & 1 & 1 & 1 \\ e^{j\phi_1} & e^{j\phi_2} & e^{j\phi_3} & e^{j\phi_4} \\ e^{\pm j2\phi_1} & e^{\pm j2\phi_2} & e^{\pm j2\phi_3} & e^{\pm j2\phi_4} \end{bmatrix} \mathbf{y}^{(4)} = \begin{bmatrix} e^{-j\phi_5} \\ 1 \\ e^{j\phi_5} \\ e^{\pm j2\phi_5} \end{bmatrix}. \tag{B.2}$$

Recall that $\sin\phi_j = \frac{1}{2j}[e^{j\phi_j} - e^{-j\phi_j}]$, $\cos\phi_j = \frac{1}{2}[e^{j\phi_j} + e^{-j\phi_j}]$, for $j = 1, \ldots, 5$, it then follows that

$$\begin{bmatrix} 1 & 1 & 1 & 1 \\ \cos\theta\sin\phi_1 & \cos\theta\sin\phi_2 & \cos\theta\sin\phi_3 & \cos\theta\sin\phi_4 \\ \sin\theta\sin\phi_1 & \sin\theta\sin\phi_2 & \sin\theta\sin\phi_3 & \sin\theta\sin\phi_4 \\ \cos\phi_1 & \cos\phi_2 & \cos\phi_3 & \cos\phi_4 \\ e^{\pm j\phi_1} & e^{\pm j\phi_2} & e^{\pm j\phi_3} & e^{\pm j\phi_4} \\ e^{\pm j\phi_1}\cos\theta\sin\phi_1 & e^{\pm j\phi_2}\cos\theta\sin\phi_2 & e^{\pm j\phi_3}\cos\theta\sin\phi_3 & e^{\pm j\phi_4}\cos\theta\sin\phi_4 \\ e^{\pm j\phi_1}\sin\theta\sin\phi_1 & e^{\pm j\phi_2}\sin\theta\sin\phi_2 & e^{\pm j\phi_3}\sin\theta\sin\phi_3 & e^{\pm j\phi_4}\sin\theta\sin\phi_4 \\ e^{\pm j\phi_1}\cos\phi_1 & e^{\pm j\phi_2}\cos\phi_2 & e^{\pm j\phi_3}\cos\phi_3 & e^{\pm j\phi_4}\cos\phi_4 \end{bmatrix} \mathbf{y}^{(4)} = \begin{bmatrix} 1 \\ \cos\theta\sin\phi_5 \\ \sin\theta\sin\phi_5 \\ \cos\phi_5 \\ e^{\pm j\phi_5} \\ e^{\pm j\phi_5}\cos\theta\sin\phi_5 \\ e^{\pm j\phi_5}\sin\theta\sin\phi_5 \\ e^{\pm j\phi_5}\cos\phi_5 \end{bmatrix}.$$

(B.3)

Hence linear dependent are the five virtual steering vectors. Thus, virtual MUSIC cannot uniquely separate four signals that obey condition (C.2), since one can find in the virtual array manifold another virtual steering vectors that may intersect the four-dimensional signal subspace.

Similarly, we can demonstrate that any four signals satisfying condition (C.3) cannot be uniquely resolved by the virtual MUSIC.

Acknowledgment

This work was supported by the National Natural Science Foundation of China under Grant Nos. 60602037 and 60672084.

References

[1] A. Nehorai, E. Paldi, Acoustic vector-sensor array processing, IEEE Trans. Signal Process. 42 (1994) 2481–2491.
[2] M. Hawkes, A. Nehorai, Acoustic vector-sensor beamforming and Capon direction estimation, IEEE Trans. Signal Process. 46 (1998) 2291–2304.
[3] M. Hawkes, A. Nehorai, Acoustic vector-sensor processing in the presence of a reflecting boundary, IEEE Trans. Signal Process. 48 (2000) 2981–2993.
[4] K.T. Wong, M.D. Zoltowski, Root-MUSIC-based azimuth-elevation angle-of-arrival estimation with uniformly spaced but arbitrarily oriented velocity hydrophones, IEEE Trans. Signal Process. 47 (1999) 3250–3260.
[5] P. Tichavský, K.T. Wong, M.D. Zoltowski, Near-field/far-field azimuth and elevation angle estimation using a single vector hydrophone, IEEE Trans. Signal Process. 49 (2001) 2498–2510.
[6] K.T. Wong, M.D. Zoltowski, Closed-form underwater acoustic direction-finding with arbitrarily spaced vector hydrophones at unknown locations, IEEE J. Ocean. Eng. 22 (1997) 649–658.
[7] K.T. Wong, M.D. Zoltowski, Extended-aperture underwater acoustic multisource azimuth/elevation direction-finding using uniformly but sparsely spaced vector hydrophones, IEEE J. Ocean. Eng. 22 (1997) 659–672.
[8] K.T. Wong, M.D. Zoltowski, Self-initiating MUSIC-based direction finding in underwater acoustic particle velocity-field beamspace, IEEE J. Ocean. Eng. 25 (2000) 262–273.
[9] B. Hochwald, A. Nehorai, Identifiability in array processing models with vector-sensor applications, IEEE Trans. Signal Process. 44 (1996) 83–95.
[10] P. Chargé, Y. Wang, J. Saillard, A non-circular sources direction finding method using polynomial rooting, Signal Process. 81 (2001) 1765–1770.
[11] M. Haardt, F. Römer, Enhancements of unitary ESPRIT for non-circular sources, in: Proc. ICASSP, 2004, pp. 101–104.
[12] J.P. Delmas, Stochastic Cramér–Rao bound for noncircular signals with application to DOA estimation, IEEE Trans. Signal Process. 52 (2004) 3192–3199.
[13] H. Abeida, J.P. Delmas, Gaussian Cramer–Rao bound for direction estimation of non-circular signals in unknown noise fields, IEEE Trans. Signal Process. 53 (2005) 4610–4618.
[14] T. Shan, M. Wax, T. Kailath, On spatial smoothing for direction-of-arrival estimation of coherent signals, IEEE Trans. Acoust. Speech Signal Process. 33 (1985) 806–811.
[15] R.O. Schmidt, Multiple emitter location and signal parameter estimation, IEEE Trans. Antennas Propagat. 34 (1986) 276–280.
[16] J. Li, Improved angular resolution for spatial smoothing techniques, IEEE Trans. Signal Process. 40 (1992) 3078–3081.
[17] R. Roy, T. Kailath, ESPRIT—Estimation of signal parameters via rotational invariance techniques, IEEE Trans. Acoust. Speech Signal Process. 37 (1989) 984–995.
[18] E. Gónen, J.M. Mendel, Applications of cumulants to array processing—Part III: Blind beamforming for coherent signals, IEEE Trans. Signal Process. 45 (1997) 2252–2264.
[19] A. Nehorai, E. Paldi, Vector-sensor array processing for electromagnetic source localization, IEEE Trans. Signal Process. 42 (1994) 376–398.
[20] M. Hawkes, A. Nehorai, Acoustic vector-sensor correlations in ambient noise, IEEE J. Ocean. Eng. 26 (2001) 337–347.
[21] Q. Wu, K.M. Wong, UN-MUSIC and UN-CLE: An application of generalized correlation analysis to the estimation of the directions of arrival of signals in unknown correlated noise, IEEE Trans. Signal Process. 42 (1994) 2331–2343.
[22] B. Friedlander, A.J. Weiss, Direction finding using noise covariance modeling, IEEE Trans. Signal Process. 43 (1995) 1557–1567.
[23] M. Pesavento, A.B. Gershman, Maximum-likelihood direction of arrival estimation in the presence of unknown nonuniform noise, IEEE Trans. Signal Process. 49 (2001) 1310–1324.
[24] M.C. Dogan, J.M. Mendel, Applications of cumulants to array processing—Part II: Non-Gaussian noise suppression, IEEE Trans. Signal Process. 43 (1995) 1663–1676.
[25] M. Viberg, P. Stoica, B. Ottersten, Array processing in correlated noise fields on instrumental variables and subspace fitting, IEEE Trans. Signal Process. 43 (1995) 1187–1199.
[26] K.-C. Tan, K.-C. Ho, A. Nehorai, Uniqueness study of measurements obtainable with arrays of electromagnetic vector sensors, IEEE Trans. Signal Process. 44 (1996) 1036–1039.

[27] M. Stojanovic, Recent advances in high-speed underwater acoustic communications, IEEE J. Ocean. Eng. 21 (1996) 125–136.
[28] E. Petit, G. Jourdain, An efficient self-recovering adaptive algorithm for BPSK signals transmitted through underwater acoustic channels, in: Proc. ICASSP, 1995, pp. 3159–3162.
[29] M. Stojanovic, L. Freitag, Multichannel detection for wideband underwater acoustic CDMA communications, IEEE J. Ocean. Eng. 31 (2006) 685–695.

Yougen Xu received the M.S. and Ph.D. degrees from Beijing Institute of Technology (BIT), Beijing, China, in 2001 and 2004, respectively, both in electronic engineering.

In September 1998, he joined the Division of Signal and Image Processing Laboratory, BIT, where he has been involved in projects related to direction finding, digital beamforming, and blind source extraction with advanced vector-sensors. Since August 2004, he has been with the Department of Electronic Engineering, BIT, where he is now an Associate Professor. His research interests are mainly in the area of vector array signal processing, sensor network, regularization methods and applications in sensor array signal processing, biomedical digital signal processing, and space–time adaptive processing.

Zhiwen Liu received the B.S. degree from Xidian University, Xi'an, China, in 1983, and the M.S. and Ph.D. degrees from Beijing Institute of Technology (BIT), Beijing, China, in 1986 and 1989, respectively, all in electronic engineering.

Since 1989, he has been with the Department of Electronic Engineering, BIT, where he is currently a Professor of signal processing and imaging techniques. His research interests include radar imaging, detection and estimation theory, video image processing, array signal processing with applications in communication, and radar and life informatics. Dr. Liu is the co-editor of 1996 CIE International Conference of Radar Proceedings. He received the 1995 Distinguished Younger Teacher Award from the Beijing Municipal Government, and won the Higher Education Teaching Award from the Beijing Municipal Government in 2001. He is a Senior Member of the Chinese Institute of Electronics (CIE).